

ENCLOSURE 2

MFN 09-749

Additive Fuel Pellets for GNF Fuel Designs, NEDO-33406,
Revision 2, December 2009

Non-Proprietary Information

IMPORTANT NOTICE

This is a non-proprietary version of NEDC-33406P, Revision 2, which has the proprietary information removed. Portions of the document that have been removed are indicated by white space with an open and closed bracket as shown here [[]].



Global Nuclear Fuel

A Joint Venture of GE, Toshiba, & Hitachi

Global Nuclear Fuel

NEDO-33406

Revision 2

Class I

DRF Section 0000-0109-9758-R0

December 2009

NON-PROPRIETARY INFORMATION

Licensing Topical Report

Additive Fuel Pellets for GNF Fuel Designs

COPYRIGHT 2009 GLOBAL NUCLEAR FUELS-AMERICAS, LLC

ALL RIGHTS RESERVED

INFORMATION NOTICE

This is a non-proprietary version of the document NEDC-33406P, Revision 2, which has the proprietary information removed. Portions of the document that have been removed are indicated by an open and closed bracket as shown here [[]].

IMPORTANT NOTICE REGARDING CONTENTS OF THIS REPORT

PLEASE READ CAREFULLY

The information contained in this document is furnished for the purpose of obtaining NRC approval of NEDC-33406P, Additive Fuel Pellets for GNF Fuel Designs. The only undertakings of Global Nuclear Fuel-Americas, LLC (GNF) with respect to information in this document are contained in contracts between GNF and its customers, and nothing contained in this document shall be construed as changing those contracts. The use of this information by anyone other than those participating entities and for any purposes other than those for which it is intended is not authorized; and with respect to any unauthorized use, GNF makes no representation or warranty, and assumes no liability as to the completeness, accuracy, or usefulness of the information contained in this document.

TABLE OF CONTENTS

	Page
1.0 Introduction	1-1
2.0 Material Properties	2-1
2.1 Microstructure.....	2-1
2.2 Melting Temperature	2-8
2.2.1 Overview.....	2-8
2.2.2 PRIME Approach.....	2-11
2.2.3 Model Correlation to Experimental Data.....	2-14
2.3 Theoretical Density.....	2-18
2.3.1 Overview.....	2-18
2.3.2 PRIME Approach.....	2-18
2.4 Thermal Expansion	2-19
2.4.1 Overview.....	2-19
2.4.2 PRIME Approach.....	2-19
2.5 Thermal Conductivity	2-22
2.5.1 Overview.....	2-22
2.5.2 PRIME Approach.....	2-22
2.5.3 Model Correlations to Experimental Data	2-25
2.6 Grain Size and Growth	2-26
2.6.1 Overview.....	2-26
2.6.2 PRIME Approach.....	2-26
2.7 Stored Energy	2-28
2.7.1 Overview.....	2-28
2.7.2 PRIME Approach.....	2-28
2.8 Creep.....	2-30
2.8.1 Overview.....	2-30
2.8.2 Prime Approach	2-31
2.8.3 Model Correlations to Experimental Data	2-33
2.9 Yield Stress.....	2-35
2.10 Modulus of Elasticity.....	2-37
2.11 Strain Hardening Coefficient and Tangent Modulus.....	2-39
2.12 Plastic Poisson's Ratio.....	2-40
2.13 Cumulative Exposure.....	2-41
2.14 Effect of Additive on the High Burn-up Fuel Pellet Rim Structure	2-42
3.0 Behavioral Assessment	3-1
3.1 Washout Characteristics	3-1

NEDO-33406 REVISION 2
NON-PROPRIETARY INFORMATION

3.2	Fuel Melting.....	3-8
3.3	Reactivity Insertion Accident (RIA) Characteristics.....	3-12
3.4	In-Reactor Densification.....	3-14
3.5	Effect on Alternate Source Term.....	3-14
3.6	Long Term Fuel Storage.....	3-16
4.0	Qualification Data.....	4-1
4.1	Qualification Dataset.....	4-1
4.1.1	[[]] – Halden Ramp Tests.....	4-1
4.1.2	Halden Steady-State (Thermal Rigs) Tests.....	4-2
4.1.3	[[]]-Halden Ramp Tests.....	4-2
4.1.4	NFD Halden Thermal Rig Tests.....	4-3
4.1.5	NUPEC(JNES) STEP3 LUA Tests.....	4-4
4.1.6	[[]]-LUA Tests.....	4-4
4.1.7	PRIME Qualification Results.....	4-5
4.2	PRIME Qualification Conclusions.....	4-13
5.0	Licensing Criteria Assessment.....	5-1
5.1	Fuel Melting.....	5-1
5.2	Fuel Rod Internal Pressure.....	5-3
5.3	Cladding Plastic Strain.....	5-4
5.4	Cladding Fatigue plus Creep Rupture Limit.....	5-6
5.5	Cladding Creep Collapse.....	5-7
5.6	LOCA\Stability\Core Transients.....	5-7
5.7	Impact on Nuclear Design Requirements.....	5-10
5.8	Licensing Criteria Conclusion.....	5-11
6.0	Operating Experience.....	6-1
6.1	Background.....	6-1
6.2	Steady State Irradiation.....	6-2
6.3	Ramp Testing and Demonstrated PCI Resistance.....	6-5
7.0	Conclusion.....	7-1
8.0	References.....	8-1

LIST OF TABLES

Table	Title	Page
Table 1-1	Additive Fuel Range to be Licensed	1-1
Table 2-1	Isothermal Additive Fuel Pellet Deformation Test Results.....	2-17
Table 3-1	[[]] Pellet Oxidation Testing Results.....	3-4
Table 3-2	Oxidation Testing Results	3-6
Table 3-3	Oxidation Testing Results from [[]] Archive Pellets	3-7
Table 3-4	Summary of Oxidation Testing Performed on Additive Fuel	3-8
Table 4-1	Model Qualification Cases from [[]] –Halden Ramp Tests	4-2
Table 4-2	Model Qualification Cases from Halden Steady-State (Thermal Rigs) Tests.....	4-2
Table 4-3	Model Qualification cases from [[]]-Halden Ramp Tests.....	4-3
Table 4-4	Model Qualification cases from NFD-Halden Thermal Rig Tests.....	4-3
Table 4-5	Model Qualification cases from NUPEC(JNES) STEP3 LUA Tests	4-4
Table 4-6	Model Qualification Cases from [[]]	4-5
Table 5-1	Fraction of Allowable Fatigue Lifetime Expended	5-6
Table 5-2	Uncertainty in Melt Margin Analysis.....	5-8
Table 5-3	Effect of Additive on High-Power Gap Conductance.....	5-8
Table 5-4	Effect of Additive on Low-Power Gap Conductance	5-9
Table 5-5	Effect of Additive on Fuel Centerline Temperature.....	5-9
Table 6-1	Summary of Segmented Rods from Halden Ramp Testing	6-8

LIST OF FIGURES

Figure	Title	Page
Figure 2-1	As-Fabricated Pellet Microstructural Comparison.....	2-2
Figure 2-2	TEM Micrograph of [[]] Additive Fuel Grain Boundary.....	2-3
Figure 2-3	Al ₂ O ₃ – UO ₂ Binary Phase Diagram.....	2-4
Figure 2-4	SiO ₂ – UO ₂ Binary Phase Diagram.....	2-5
Figure 2-5	Al ₂ O ₃ – SiO ₂ – UO ₂ Phase Diagram.....	2-5
Figure 2-6	Additive – UO ₂ Pseudo-Binary Phase Diagram [[]].....	2-6
Figure 2-7	Additive – UO ₂ Pseudo-Binary Phase Diagram [[]].....	2-7
Figure 2-8	Fuel Melting Point Calculation Example.....	2-9
Figure 2-9	Additive Fuel Melting Temperature.....	2-10
Figure 2-10	Additive Fuel Phase Diagram (Schematic).....	2-14
Figure 2-11	PRIME Liquidus / Eutectic Temperature and Experimental Data.....	2-15
Figure 2-12	PRIME Liquidus / Eutectic Temperature and Data / Error Bars.....	2-16
Figure 2-13	Thermal Expansion of Additive Fuel from Room Temperature.....	2-21
Figure 2-14	Thermal Conductivity Data for Additive Fuel.....	2-25
Figure 2-15	Steady State Creep Rates of Additive Fuel vs. Standard UO ₂	2-30
Figure 2-16	Prime Creep Calculations Vs. Data for 0.25 wt% Additive.....	2-34
Figure 2-17	Prime Creep Calculations Vs. Data for 1.0 wt% Additive.....	2-34
Figure 2-18	Prime Creep Calculations Vs. Data for 0.5 wt% Additive.....	2-35
Figure 2-19	SEM images of the amorphous-appearing structure within the initial UO ₂ grains and the presence of the initial grain boundaries in the HBS.....	2-43
Figure 3-1	Comparison of Corrosion Behavior of Synthetic vs. Natural Additives.....	3-3
Figure 3-2	Circumferentially Oriented Flaws in [[]].....	3-5
Figure 3-3	Representative Thermal-Mechanical Envelope for GNF2.....	3-10
Figure 3-4	Limiting Case of Fuel Fraction Above Eutectic Temperature.....	3-10
Figure 3-5	Region of Fuel Above Eutectic at Limiting LHGR and Exposure.....	3-11
Figure 3-6	RIA Testing Results.....	3-13
Figure 4-1	Predicted versus Measured Fuel Temperature.....	4-6
Figure 4-2	Predicted/Measured Fuel Temperature versus Exposure.....	4-7
Figure 4-3	Predicted versus Measured Fission Gas Release.....	4-8
Figure 4-4	Predicted/Measured Fission Gas Release versus Exposure.....	4-9
Figure 4-5	Predicted versus Measured Fuel Rod Internal Pressure.....	4-10
Figure 4-6	Predicted-Measured Rod Internal Pressure versus Exposure.....	4-11
Figure 4-7	Predicted versus Measured Cladding Diametral Strain.....	4-12

NEDO-33406 REVISION 2
NON-PROPRIETARY INFORMATION

Figure 4-8	Predicted-Measured Cladding Diametral Strain.....	4-13
Figure 5-1	Effect of Additive on Fuel Melting	5-2
Figure 5-2	Effect of Additive on Fuel Rod Internal Pressure	5-4
Figure 5-3	Effect of Additive on Cladding Permanent Strain.....	5-5
Figure 6-1	Additive Fuel Operating History Summary	6-1
Figure 6-2	Additive Fuel Ramp Testing Results.....	6-5
Figure 6-3	Temperature Gradient of Rod Segment [[]].....	6-9
Figure 6-4	Temperature Gradient of Rod Segment [[]].....	6-10
Figure 6-5	Temperature Gradient of Rod Segment [[]].....	6-11

EXECUTIVE SUMMARY

GNF desires to introduce aluminosilicate additive fuel pellets into GNF fuel products to increase fuel reliability and operational flexibility of nuclear fuel bundles and cores. This document provides the technical justification to deploy additive fuel in [[]] using [[]] additives at concentrations of up to [[]] by weight and SiO₂:Al₂O₃ ratios in the range of [[]] by weight. Ramp testing has demonstrated additive is effective at concentrations as low as [[]] by weight UO₂ and that additive fuel can survive in the range in which 95% of non-barrier standard fuel would fail. At the small concentrations being proposed, the additive has minimal effect on the thermal-mechanical properties of the fuel at normal operating conditions.

REVISIONS

Number	Purpose of Revision
0	Initial Issue.
1	Corrected significant figures for ASTM concentration in Table 1-1, corrected composition low end in Table 1-1 and Section 7.
2	Editorial changes and clarifications for sections 2.1, 2.2, 3.2 and 5.1. Added section 2.14 on High Burn-up Structure (HBS). Inserted new section 5.7 on nuclear licensing effects and renumbered remaining section. Added discussion to section 6.3 on fuel operation above eutectic.

1.0 INTRODUCTION

Additive fuel pellet technology has been investigated since 1976. At that time, a comprehensive program was initiated to characterize and test additive fuel, with a specific focus on conditions where pellet clad interaction (PCI) occurs. As part of this program, additive fuels were characterized, and material properties were determined for implementation into thermal-mechanical methods. Several lead test assemblies and segmented rods were inserted into power reactors in both the US and abroad. Instrumented fuel assemblies were inserted into a test reactor to develop thermal and mechanical data to support design and licensing. A series of tests were performed to characterize the reactivity initiated accident performance of additive fuels. More recently, additive fuel Lead Use Assemblies (LUAs) have been deployed in two foreign reactors to provide irradiated material for studying high exposure effects. [[

]]

[[

]] The table below summarizes the range of concentration, composition and product applicability of additive fuel to be approved by acceptance of this LTR.

Additive Fuel Range of Applicability			
	Concentration wt%	Composition SiO ₂ : Al ₂ O ₃ by wt	Fuel Design
Derived from ASTM C776-00 Impurity Limit	[[]]	[[]]	N/A
Target Range	[[]]	[[]]	GE14, GNF2, new

Table 1-1 Additive Fuel Range to be Licensed

The scope of this licensing topical report will focus on relevant fuel material properties and in-core behavioral characteristics that are affected by the addition of additive and demonstrate the negligible effects on licensing safety limits with additive fuel pellets. This document will serve as a supplement to the PRIME licensing topical reports [References 1, 2, and 3] previously submitted to further support the models technical basis and qualification to data not shown in the previous submittals. By agreement with NRC staff, the submission and review of PRIME was

NEDO-33406 REVISION 2
NON-PROPRIETARY INFORMATION

limited to non-additive fuel and it is this topical report that requests approval of PRIME use with additive fuel. No changes to any of the additive fuel models in PRIME previous submittals are proposed with this topical report.

2.0 MATERIAL PROPERTIES

In the planned additive concentration and composition ranges, the material properties of additive fuel and standard, non-additive fuel are generally similar and in some cases the same. However, several fuel material properties differ between additive fuel and standard, non-additive fuel and these properties are outlined in this section. This section also includes a description of how these properties are handled in the PRIME thermal-mechanical code. Some calculations in the PRIME methodology require gadolinia content as an input. [[

]]

The properties discussed in this section are melting, density, thermal expansion, thermal conductivity, grain size and grain growth, stored thermal energy, creep, yield strength, elastic modulus, strain hardening coefficient and tangent modulus, plastic Poisson's ratio, and swelling. Due to the importance of microstructure to the material properties and irradiation behavior, a general description of the microstructure of additive fuel will also be discussed.

2.1 MICROSTRUCTURE

Although microstructural evolution, other than grain growth, is not explicitly modeled in PRIME, the microstructure of additive fuel can differ from that of standard UO_2 fuel, and those differences prove to be the primary driver of the materials properties that differ in PRIME.

As shown in Figure 2-1, the as-fabricated pellet microstructure consists principally of a single phase UO_2 with a minor additive "phase" residing at the UO_2 grain boundaries. This additive phase can consist of additional phases [[

]] For simplicity,
these non- UO_2 grain boundary-resident phases are collectively called the additive phase.

[[

]]

Figure 2-1 As-Fabricated Pellet Microstructural Comparison

During fabrication, the additive phase uniformly covers the grain boundaries, with excess additive tending to accumulate preferentially at grain edges and corners, an effect seen in Figure 2-1. The thickness of additive phase coating grain boundary faces [[
]], as shown in Figure 2-2.

[[

]]

Figure 2-2 TEM Micrograph of [[Additive Fuel Grain Boundary

This microstructure evolves further upon significant heating in operation. Typically, single-phase ceramic materials such as UO_2 of reasonably high purity exhibit what can be considered discrete melting temperatures, above which the material is all or nearly all liquid and below which the material is all or nearly all solid. [[

]]

The effect is that, during a temperature increase, at a critical temperature (the eutectic temperature) below the UO_2 melting temperature, any crystalline silica vitrifies. Upon further increase in temperature a larger volume fraction of the fuel becomes vitreous as the solubility of alumina and urania in this phase increases, dissolving more alumina and urania into the vitreous solution until the liquidus temperature is reached and the vitreous fraction of additive fuel is

100%, at which point the fuel can accurately be described as fully liquid. Such behavior is typical for any vitreous or low melting point impurity which forms a eutectic with UO_2 , a category which includes both pure alumina (Al_2O_3) and silica (SiO_2) as well as other impurities routinely found in fuel pellets at small but measurable levels. Such behavior can be conceptualized with equilibrium phase diagrams, though they fail to capture some of the complexities introduced with non-equilibrium vitreous phases. Figures 2-3 and 2-4 show these binary phase diagrams. In these diagrams, equilibrium vitreous phases are described as “liquid” in reference to their long range crystalline order, in contrast to their viscosity or mechanical properties. This distinction is clarified here because it is a fuel’s viscosity and mechanical properties, rather than long-range order, that most affect safety related behavior.

[[

]]

Figure 2-3 Al_2O_3 – UO_2 Binary Phase Diagram

[[

]]

Figure 2-4 $\text{SiO}_2 - \text{UO}_2$ Binary Phase Diagram

Each of the binary phase diagrams in Figures 2-3 and 2-4 are represented on one of the three edges of the ternary phase diagram in Figure 2-5. The interior of the ternary phase diagram contains contour lines showing the liquidus surface, with the heavy lines denoting the ternary loci of binary eutectic points.

[[

]]

Figure 2-5 $\text{Al}_2\text{O}_3 - \text{SiO}_2 - \text{UO}_2$ Phase Diagram

A pseudo-binary diagram similar to those of Figures 2-3 and 2-4 can be determined for the additive – UO₂ system for any discrete additive composition (silica:alumina ratio). Such a diagram is a slice through the ternary diagram of Figure 2-5 connecting the additive composition of interest on the Al₂O₃ - SiO₂ line to the UO₂ corner point. Figures 2-6 and 2-7 are two such phase diagrams, presented in schematic form, which represent the compositions with which GNF has the most experience and approximating the bounding compositions under consideration. Figure 2-6 shows the phase diagram for additive fuel at a silica:alumina ratio of [[

]]

[[
Figure 2-6 Additive – UO₂ Pseudo-Binary Phase Diagram [[
]]

[[
]]
Figure 2-7 Additive – UO₂ Pseudo-Binary Phase Diagram [[
]]

[[

]] The peritectic temperature, at which vitreous aluminosilicate becomes thermochemically stable upon heating, is described in PRIME (Section 2.2.2) and is [[]], above which only the vitreous additive and crystalline UO₂ phases are assumed to exist for the purposes of the calculation. [[

]] While this critical temperature has been verified experimentally (see Section 2.2.3) there is some solid mullite phase predicted to exist between the peritectic temperature and approximately [[]] in the case of the targeted composition region for which no credit is taken for decreased total vitreous phase content. In practice, the melting transition occurs over the temperature range from the ternary peritectic of [[]] to the liquidus, the temperature of which varies as a function of additive content and at a concentration of zero is equal to the melting point of pure

UO₂. For this reason, the peritectic temperature is referred to as the eutectic temperature throughout the text of this Report and in PRIME documentation.

2.2 MELTING TEMPERATURE

2.2.1 OVERVIEW

Fuel melting properties are considered in this section, while predictions of melting during normal operating conditions is addressed in Section 3.2 and during AOOs in Section 5.1. Melting of the fuel pellet is avoided to ensure that fuel does not relocate within the fuel pin under the force of gravity; that excess fission gas release does not occur; and that there is no deleterious reaction between molten fuel and the fuel rod cladding. Because the additive phase does not exhibit a congruent melting phase transition, a melting point definition is provided to ensure that each of these requirements are met at any temperature below the melting point so defined.

Of the above requirements, fuel relocation is most limiting for additive fuel. As shown in Section 3.2, the region of pellets exposed to cladding material is not hot enough during operation to permit contact of molten material with cladding. [[

]] As discussed in Section 2.1, the melting temperature of additive fuel is not a clearly defined phase transition point as in pure UO₂, and is not associated with the distinct phase transition of melting. Rather, with increasing temperature, there is a gradual dissolution of fuel volume into a vitreous phase and a gradual decrease in the viscosity of the vitreous phase. This transition occurs over the temperature range from the eutectic temperature to the liquidus temperature that defines the temperature where the material is 100% liquid for a given composition. The mechanical properties, which govern the ability of the fuel to relocate, change gradually over this temperature range and the risk of fuel relocation is expected somewhere within it. Thus, for the purposes of additive fuel pellets, an effective melting temperature is defined to ensure the fuel pellets do not relocate during normal operations including postulated AOOs. This effective melting temperature is a temperature below the liquidus where the fuel pellet deforms similar to melting for pure UO₂ [[

]] Because this occurs at a lower temperature than the liquidus limit and widespread relocation (as used in standard UO₂), [[

]] Furthermore, the resistance of the vitreous phase to deformation varies with temperature, but in PRIME it is assumed to have no contribution to the resistance to deformation at temperatures above the eutectic temperature. Because of this, at temperatures above the eutectic the vitreous phase is conservatively considered a liquid for mechanical purposes and in that context the terms are used interchangeably.

[[]] was investigated experimentally (see section 2.2.3) for additive fuel, and it was found that [[

]]. The corresponding temperature can in turn be derived by [[]]

[[]]

Figure 2-8 Fuel Melting Point Calculation Example

An example is given below to illustrate. Consider a pellet containing [[]] additive with zero exposure. In this example [[]]

]]. The melting point can then be calculated using [[]], the PRIME value of which is plotted in Figure 2-8 in black, at [[]] additive, yielding a result of [[]]. In this example, the presence of [[]] additive results in a depression of [[]] from the non-additive melting point. In the proposed implementation, [[]], which can be converted to [[]] such as that used above by using the relationships in the following section. This approach yields a melting point curve, varying with temperature, as shown in Figure 2-9. This figure, plotted for zero exposure and no gadolinia content, shows the melting point depression at additive concentrations of interest, as well as the conservative nature of the defined melting point with respect to the liquidus. In this case, the melting point refers not to the crystallinity of the fuel but to a conservative assessment of the pellet resistance to macroscopic deformation; as such it is an effective melting point, though not the temperature at which fully-liquid behavior is observed.

[[]]

Figure 2-9 Additive Fuel Melting Temperature

2.2.2 PRIME APPROACH

In PRIME, the fuel melting temperature model is developed similarly to the fuel thermal conductivity model (see Section 2.5). The relation for the melting temperature of UO_2 is developed and then extended to include the effects of burn up, gadolinia and additive, based upon thermal arrest measurement data for UO_2 , $(\text{U,Gd})\text{O}_2$ and UO_2 containing additive. The resulting fuel melting temperature relation is described in detail below.

[[

NEDO-33406 REVISION 2
NON-PROPRIETARY INFORMATION

NEDO-33406 REVISION 2
NON-PROPRIETARY INFORMATION

]].

[[

]]

Figure 2-10 Additive Fuel Phase Diagram (Schematic)

2.2.3 MODEL CORRELATION TO EXPERIMENTAL DATA

Determination of the melting point [[

these components, [[]] Because of the importance of

[[

]]

]]

Figure 2-11 PRIME Liquidus / Eutectic Temperature and Experimental Data

[[

]]

Figure 2-12 PRIME Liquidus / Eutectic Temperature and Data / Error Bars

Figure 2-12 shows the same data as Figure 2-11, but includes average values for each point along with error bars corresponding to the sum of the standard deviation of the individual measurements and the estimated temperature measurement error based on testing against calibration standards. The correlation shown in these two figures represents the ability of PRIME to provide an accurate prediction of [[

]]

The second component, [[]], was determined experimentally. The assumption in PRIME [[

]]

[[

]]

Table 2-1 Isothermal Additive Fuel Pellet Deformation Test Results

Clearly the fuel retains resistance to slumping at temperatures well in excess of the eutectic temperature because all fuel is sintered above the eutectic temperature and the pellets exhibit no measurable deformation. However, more detailed studies were conducted to determine more precisely how much higher than the eutectic the temperature can go before resulting in macroscopic deformation. In these studies additive test pellets were exposed [[

]]

These data show that [[

]]

The [[

]]

2.3 THEORETICAL DENSITY

2.3.1 OVERVIEW

The room temperature theoretical density of additive fuel differs slightly from standard UO₂ due to the higher density UO₂ displaced by the lower density additive phase. The theoretical density is calculated based [[]].

2.3.2 PRIME APPROACH

The theoretical density of (U,Gd)O₂ additive fuel is given by [[

]]

(2-7)

2.4 THERMAL EXPANSION

2.4.1 OVERVIEW

[[

]] This difference is insignificant for the proposed additive formulations [[

]], as shown in

Section 2.4.2. [[

]] Above the

eutectic temperature there is an increasing fraction of lower density liquid phase present, but this liquid phase increases in [[

]] This

is calculated on an *a priori* basis using fundamental properties of the additive phase. [[

]], the net effect is generally negligible or very small.

2.4.2 PRIME APPROACH

The thermal expansion equivalent strain of a fuel pellet ring is assumed isotropic and given by

[[

NEDO-33406 REVISION 2
NON-PROPRIETARY INFORMATION

]]

Figure 2-13 shows a comparison of the PRIME outputs for thermal expansion of unirradiated additive fuel at a concentration of [[]] versus that of standard UO₂ fuel.

[[

]]

Figure 2-13 Thermal Expansion of Additive Fuel from Room Temperature

2.5 THERMAL CONDUCTIVITY

2.5.1 OVERVIEW

Because the thermal conductivity of the additive phase is lower than that of pure UO_2 , the thermal conductivity of additive fuel is slightly lower than that of conventional fuel. This effect is highly dependent on the concentration of additive, and has been measured for high additive concentrations [[], though at the concentrations of interest there is very little effect. The thermal conductivity decrease is most pronounced at lower temperatures and low burn ups. At higher temperatures, the phonon scattering penalty suffered by the additive phase becomes less important as radiative heat transfer predominates, and at higher burnups the addition of phonon scattering sites and features has a greater influence on the previously low entropy UO_2 lattice than the glassy additive phase. Thus, at high temperatures and higher burn up the additive fuel thermal conductivity further approaches that of standard UO_2 .

2.5.2 PRIME APPROACH

In PRIME, the fuel thermal conductivity model is developed for UO_2 and then extended to include the effects of burn up, gadolinia and additive. To permit explicit treatment of the observed burn up dependency, the phonon contribution to the thermal conductivity of UO_2 is based upon the Klemens model. The burn up dependency is included by modifying the phonon term to account for the defect concentration due to burn up. The modification includes the effect of defect recovery due to thermal annealing. The gadolinia dependency is similarly addressed by additionally modifying the phonon term to account for the defect concentration due to gadolinia. Finally, the effects of addition of additive are explicitly addressed. The resulting fuel thermal conductivity relation is described in detail below.

[[

]]

NEDO-33406 REVISION 2
NON-PROPRIETARY INFORMATION

The results of these tests are reflected in PRIME through the following thermal conductivity relations. These relations are presented in SI units for convenience. The relations are converted to English units for use in PRIME (1 BTU=0.2931 Watt-hr, 1 ft=0.3048 m, and 1 °R=0.5556 K).

For $T \leq T_{EUT}$

$$K = \left[\quad \quad \quad \right] \quad (2-11)$$

For $T > T_{EUT}$

$$K = \left[\quad \quad \quad \right] \quad (2-12)$$

Where

K = Fuel thermal conductivity (W/mK)

$\left[\right]$

NEDO-33406 REVISION 2
NON-PROPRIETARY INFORMATION

]]

2.5.3 MODEL CORRELATIONS TO EXPERIMENTAL DATA

Laboratory measurements of thermal conductivity were performed on test pellets using [[
]] and the results are plotted in Figure 2-14 against the corresponding PRIME
predictions. These pellets were fabricated with [[
]] at the concentrations indicated.

[[

]]

Figure 2-14 Thermal Conductivity Data for Additive Fuel

The effect of additive on the thermal conductivity of fuel is small, even at the tested concentrations, which are greater than those under consideration for use.

2.6 GRAIN SIZE AND GROWTH

2.6.1 OVERVIEW

Grain size and growth are important because of the tendency for larger grains to suppress fission gas release at low and moderate exposures. Both the initial grain size and grain growth during operation [[

]] The initial grain size for additive fuel can be significantly larger than that of standard UO₂, and this phenomenon is reflected in the generic grain growth approach and implemented by having separate design basis values for the grain sizes of additive fuel and non-additive fuel. [[

]]

2.6.2 PRIME APPROACH

Grain growth is given by

[[

NEDO-33406 REVISION 2
NON-PROPRIETARY INFORMATION

]]

For application in PRIME, grain growth is calculated for each pellet ring. An arithmetic mean of the temperatures at the inner and outer ring boundaries is used. Additionally, a limiting grain size is defined to avoid a potential non-conservative under prediction of fission gas release fraction. No grain growth is calculated when the current grain diameter is equal to or larger than [[]].

2.7 STORED ENERGY

2.7.1 OVERVIEW

The fuel stored thermal energy is modified slightly by the presence of additive using [[

]] reflecting the stored energy of pure UO_2 and that of pure additive phase. Because the range of relative quantities of additive phase under consideration is very small, the effect is small. This approach is used up to the melting point, [[

]]. Above the melting point it is assumed that there is a step change in the heat capacity [[]]. While this only approximates the complex melting behavior of additive fuel, because the model is weighted by the annular ring volume and the total liquid fraction in a pellet is very small in even the most extreme AOOs intended to be analyzed by PRIME (see Section 3.2), the error introduced by the approximation is negligible.

2.7.2 PRIME APPROACH

In PRIME, stored energy is calculated for each pellet ring and then weighted by the annular ring volume to obtain the pellet-stored energy. For each ring the stored energy is given by

NEDO-33406 REVISION 2
NON-PROPRIETARY INFORMATION

[[

]]

2.8 CREEP

2.8.1 OVERVIEW

The steady-state creep behavior of additive fuel is [[

]] is shown in Figure 2-15, which shows PRIME calculations of steady state creep rates as a function of stress at various temperatures for both [[
]] The inputs include a fission rate of 0, [[
]]

[[

]]

Figure 2-15 Steady State Creep Rates of Additive Fuel vs. Standard UO₂

2.8.2 PRIME APPROACH

Uniaxial compression tests have been performed to determine the creep characteristics [[

]]

The results of these tests are reflected in the PRIME model through the use of a fuel pellet creep model of the form

[[

NEDO-33406 REVISION 2
NON-PROPRIETARY INFORMATION

]]

2.8.3 MODEL CORRELATIONS TO EXPERIMENTAL DATA

Uniaxial compression testing was performed on unirradiated additive fuel samples and some of the results are plotted in Figure 2-16 through Figure 2-18.

[[]]

Figure 2-16 Prime Creep Calculations Vs. Data for 0.25 wt% Additive

[[]]

Figure 2-17 Prime Creep Calculations Vs. Data for 1.0 wt% Additive

Figure 2-16 and Figure 2-17 show the steady state creep rate plotted against applied uniaxial stress at a variety of temperatures, and cover additive at concentrations of [[

]] Figure 2-18 shows the steady state creep rate plotted against temperature at a variety of applied stresses. In all of these tests, the test pellets were unirradiated fuel and the data were normalized to 95% theoretical density. The PRIME outputs use the same input parameters discussed in Section 2.8.1.

[[

]]

Figure 2-18 Prime Creep Calculations Vs. Data for 0.5 wt% Additive

2.9 YIELD STRESS

[[

]] The yield stress models described below have been developed based on mechanical testing of unirradiated additive fuel [[

]] Based upon the results, the fuel yield stress in PRIME is given by

[[

]]

2.10 MODULUS OF ELASTICITY

In modeling additive fuel there is an adjustment made to the modulus of elasticity of standard non-additive fuel to compensate for the effect of the glassy and/or liquid phase present. [[

NEDO-33406 REVISION 2
NON-PROPRIETARY INFORMATION

]]

2.11 STRAIN HARDENING COEFFICIENT AND TANGENT MODULUS

In modeling additive fuel there is an adjustment made to the strain hardening coefficient and tangent modulus of standard non-additive fuel to compensate for the effect of the glassy and/or liquid phase present. [[

]]

In PRIME, the fuel material stress-strain curve is given by the relation

[[

]] (2-31)

2.12 PLASTIC POISSON'S RATIO

In general, plastic deformation is assumed to be nondilatational, i.e. plastic deformation does not include an associated volume change. In PRIME, this assumption is applied [[

]]

2.13 CUMULATIVE EXPOSURE

Cumulative exposure is not a material property but is a parameter that affects material properties like [[

]]

2.14 EFFECT OF ADDITIVE ON THE HIGH BURN-UP FUEL PELLET RIM STRUCTURE

The additive consists of a combination of glassy and crystalline phases after sintering. It has a very high viscosity at temperatures below $\sim 1200^{\circ}\text{C}$ so that the as-sintered additive is essentially rigid despite the presence of a glassy phase. The additive remains on the grain faces during in-reactor operation, does not combine chemically with UO_2 or $(\text{U}, \text{Pu})\text{O}_2$ and is immobile at temperatures in the range where High Burn-up Structure (HBS) has been observed to form. The consequence of these conditions is that the additive is expected to remain on the boundaries of the as-sintered grains in the region of the HBS, Figure 2-19, and not diffuse into or react chemically with the recrystallized grains that comprise the HBS.

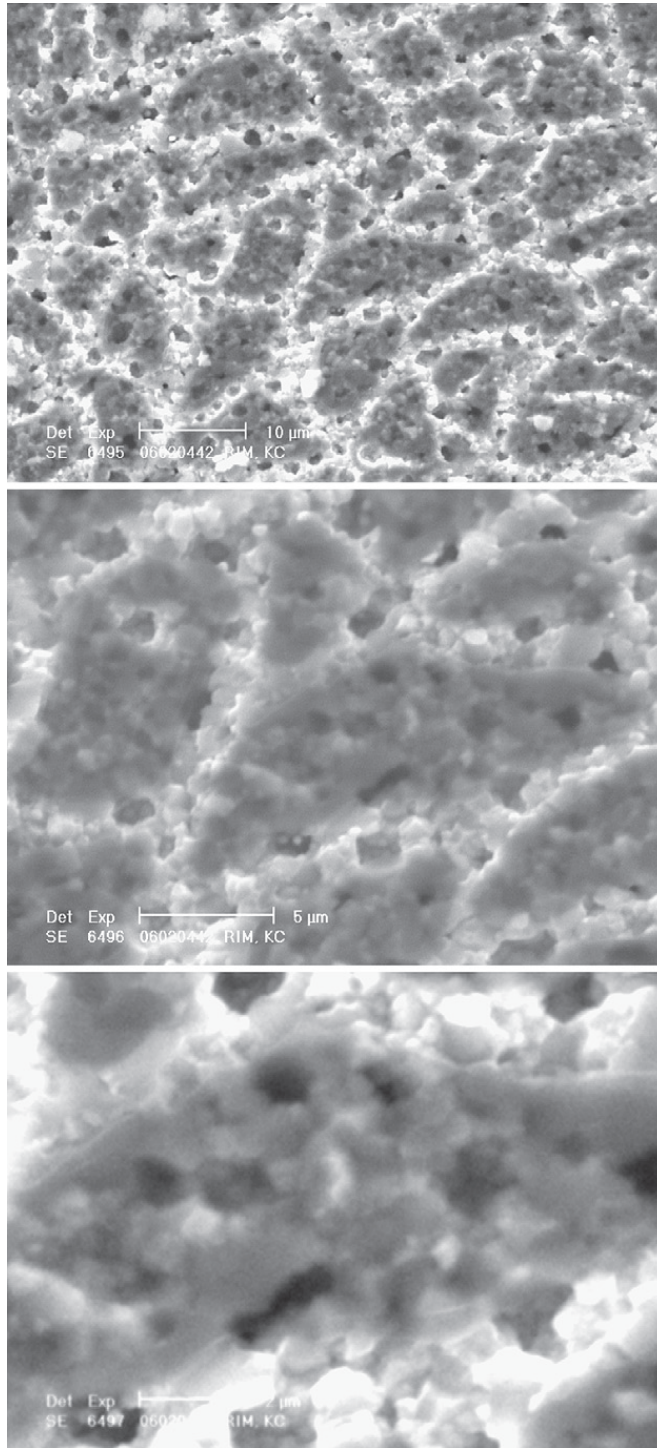


Figure 2-19 SEM images of the amorphous-appearing structure within the initial UO₂ grains and the presence of the initial grain boundaries in the HBS

The implications of the expected behavior of the Al-Si-O additive on the HBS structure are:

1. The formation of the rim structure will be suppressed by the presence of large as-sintered grains as observed in Japanese tests to pellet average exposures in excess of 80 GWd/MTU,
2. The Al-Si-O additive will not affect the formation or the properties of the HBS except as related to the size of as-sintered grains,
3. The effect of the HBS on thermal and mechanical properties will be the same in fuel with the Al-Si-O additive as in fuel without the additive and as modeled in the PRIME computer code,
4. The Al-Si-O additive is not expected to alter the storage in or the dispersal from the HBS of fission products and fuel material in the event of postulated accidents; e.g., Loss-of-Coolant-Accident (LOCA) or Reactivity Insertion Accident (RIA),
5. The post-irradiation microstructural stability and chemical properties of the HBS in pellets with the Al-Si-O additive is expected to be the same as in pellets without the additive.

In conclusion, as noted above the Al-Si-O additive of GNF resides on the as-sintered boundaries of UO_2 grains and is expected to alter the formation of the HBS structure only through the presence of larger grains; i.e., slightly suppress the formation of a HBS. The additive is insoluble in UO_2 and the mixed (U, Pu) O_2 that forms during irradiation. The mobility of the additive is sufficiently low at temperatures where the HBS has been observed that it will not diffuse or otherwise migrate into the porosity of the HBS. As a result, the Al-Si-O additive is not expected to affect the HBS or alter the behavior of the HBS with respect to in-reactor and post-irradiation performance.

3.0 BEHAVIORAL ASSESSMENT

Based upon the effects of additive on fuel pellet microstructure, at the preferred GNF additive composition and concentrations, as discussed in Section 2.0, the following characteristics are potentially impacted: washout behavior, fuel melting, RIA behavior, in-reactor densification, validity of alternate source term assumptions, and long-term fuel storage. Each effect is discussed below.

3.1 WASHOUT CHARACTERISTICS

Pellet susceptibility to oxidation in the presence of water at BWR conditions has been closely examined by GNF to evaluate the propensity for fuel washout. Over a period of more than a decade, testing has been performed on laboratory and factory produced pellets with a wide variety of additive compositions and concentrations. For those covered under the scope of this Report the test results support a conclusion that washout behavior for additive fuel is comparable to that of standard UO_2 .

The standard view of washout behavior is that after a breach of the fuel rod cladding, water is introduced to the fuel rod interior and can interact with the fuel inside. Water at BWR conditions proves mildly corrosive to UO_2 , and that corrosivity is dependent on several factors, principally the grain structure of the fuel. Testing shows that the grain boundaries are more susceptible to corrosion than grain faces, so corrosion begins at grain boundaries and proceeds along them at a faster rate than through bulk grains. For this reason, there is typically greater corrosion rates for small-grained fuel than for large grained fuel, which has a lower density of grain boundaries. Based upon this understanding of the washout phenomenon, the solubility of any material residing at the grain boundaries has the potential to have an important influence on the corrosion resistance properties of the fuel.

For the purposes of this evaluation, pellet susceptibility to oxidation was tested by [[

]] The results indicate that for the additive variation being considered, the behavior is similar to that of non-additive fuel. This

is consistent with the current understanding of the washout phenomenon. UO₂ fuel with large grains has been shown to exhibit enhanced corrosion resistance relative to standard UO₂ fuel with smaller grains due to the lower grain boundary area-to-volume ratio. The addition of additive to UO₂ fuel can result in larger grains. Accordingly, additive fuel corrosion resistance would be expected to be better than standard UO₂ fuel due to the grain size effect alone. [[

]] At the concentrations being considered, the additive glassy phase tends to accumulate in significant quantities only at the grain boundary edges and corners, with the grain boundary planes containing only a thickness [[]] as shown in Figure 2-2. [[

]] support the experimental observations that the corrosion performance is comparable to that of standard UO₂ fuel.

In tests of laboratory-prepared pellets [[

]]

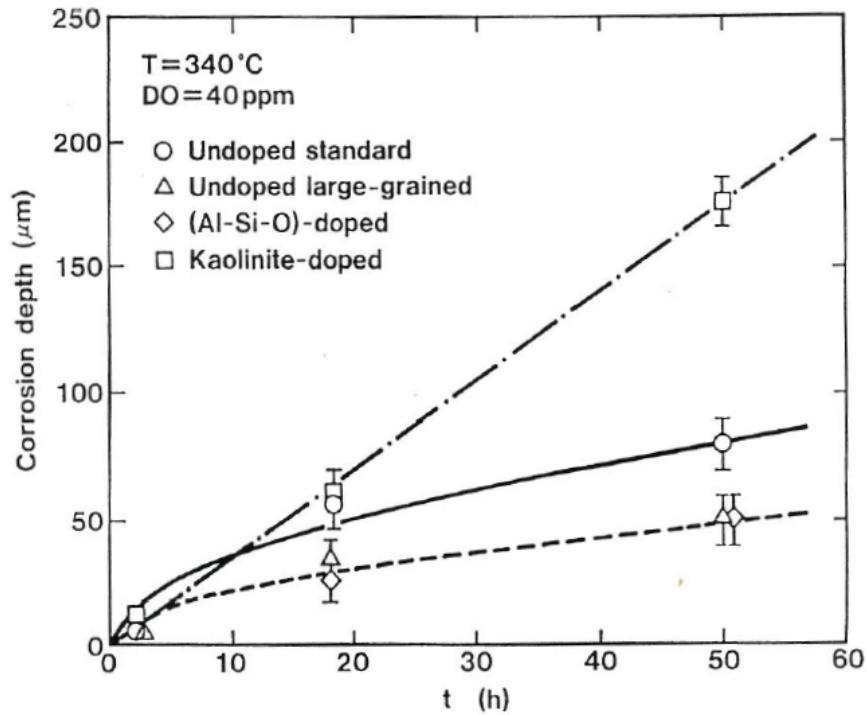


Figure 3-1 Comparison of Corrosion Behavior of Synthetic vs. Natural Additives
(Taken from K. Une, Corrosion Behavior of unirradiated Oxide Fuel in High Temperature Water, May 1995)

In addition to testing performed on laboratory pellets, archive pellets from additive LUA programs have also been evaluated. For the [[]], additive pellets were made with [[]]

]]

There was no significant difference between the corrosion resistance of additive vs. non-additive fuel once this effect was accounted for. For the original evaluation of the [[]], unirradiated archive pellets were tested [[]]

]], and the results are shown in Table 3-1.

[[

]]

Table 3-1 [[Pellet Oxidation Testing Results

[[

]] several types of sample pellets were prepared by GE Corporate Research and Development (GE-CRD) in a laboratory using

[[

]]

[[

Figure 3-2 Circumferentially Oriented Flaws in [[

]]

]]

[[

]]

NEDO-33406 REVISION 2
NON-PROPRIETARY INFORMATION

A final test of laboratory prepared pellets was performed on pellets prepared by Nippon Fuel Development (NFD) and tested by GNF. These samples were tested in the same way as the GE-CRD pellets discussed above, and the two sets of tests combine to represent the most comprehensive and carefully prepared and measured evaluation of pellet oxidation available for additive types similar to those to be used by GNF. [[

]] The results are presented in Table 3-2. Note that the GE-CRD and NFD pellets were [[
]], though the trends evident within a group of pellets are valid.

[[

]]

Table 3-2 Oxidation Testing Results

From Table 3-2, it can be seen that [[

]], and the

samples representative of the GNF-targeted additive composition [[]] and concentration [[]] actually showed improved corrosion resistance over standard UO₂.

The most recent set of oxidation tests was performed on unirradiated archive pellets fabricated for the [[]]. These pellets were the most recently factory-produced pellets tested for oxidation and are the most representative of the current GNF pellet production process. The data are presented in Table 3-3.

[[

]]

Table 3-3 Oxidation Testing Results from [[]] Archive Pellets

The additive used for the [[]] with a [[]], and corrosion testing was performed using the same [[]] method as used for the GE-CRD, NFD, and [[]] pellets. The results of the corrosion testing are consistent with prior work [[]] in that they show that the corrosion resistance of additive fuel made with [[]] additives is comparable to that of standard UO₂.

The laboratory tests as described here indicate that additive fuel pellets of the type to be used by GNF are not intrinsically more susceptible to corrosion-assisted washout than are standard UO₂ pellets.

[[

]]

Table 3-4 Summary of Oxidation Testing Performed on Additive Fuel

Table 3-4 summarizes the results of GNF testing of additive fuel corrosion behavior. It is apparent that [[]] additives offer superior oxidation resistance over [[]] additives, driving GNF's design to use only [[]] additives. [[]] additives offer comparable corrosion resistance to standard UO₂.

3.2 FUEL MELTING

In addition to the fuel melting behavior description of additive fuel contained in Sections 2.1 and 5.1, there are other considerations of the expected fuel melting behavior. One such aspect of the unique melting behavior of additive fuel is evolution of the fuel microstructure upon thermal cycling which repeatedly increases and decreases the liquid fraction in the pellets. Upon heating above the eutectic temperature, UO₂ dissolves into the vitreous phase, which then precipitates back out as UO₂ upon subsequent cooling. In laboratory testing of pellets at high additive concentrations (5000 ppm), UO₂ particles have been observed to precipitate from large islands of additive on the pellet surface upon cooling from temperatures above the eutectic temperature, indicating the possibility of microstructural evolution due to thermal cycling. However, in factory-produced pellets these additive islands at the pellet surface are not observed, nor have any UO₂ precipitates in the additive phase otherwise been observed in such pellets. Any surface

layer of additive that would be present are removed by surface grinding of the pellets, and additive islands in the pellet interior are not large enough to support this precipitation mechanism. The precipitation mechanism observed occurs by accretion of UO_2 on a nearby grain, the inverse of the dissolution process, thus resulting in a microstructure that is indistinguishable from that present before thermal cycling. Because of this, thermal cycling is not considered to have any new effect on additive fuel properties or performance.

Also of note is that the melting behavior of additive fuel exhibits similarities to that of non-additive fuel. For example, the ASTM impurity limits for aluminum and silicon are 250 and 500 wppm respectively for sintered UO_2 pellets, which corresponds to an equivalent [[

]] additive concentration of about [[

]] Even at impurity concentrations well below the ASTM impurity limit, at purity levels comparable to those seen in typical standard UO_2 pellets, there is some aluminosilicate present, and the same behavior of partial melting above the eutectic temperature is exhibited through the full range of silica:alumina ratio compositions. For example, for a “non-additive” pellet at 10% of the ASTM specification limit for aluminosilicate impurities, or an “additive” concentration of 105 wppm, the fuel melting point is depressed by 1.8 °C according to the PRIME model, [[and approximately [[

]]

Another relevant consideration is that [[described in Section 2.1, is considered conservative because temperatures [[

]] are confined to the pellet center, which makes up only a small fraction of the overall pellet volume, while the outer, cooler, region of the pellet [[including the additive phase. [[

]] Even at the limits of normal operation, only a small fraction of fuel is exposed to temperatures above the [[To illustrate this, PRIME was used to model the case of a full length rod fuel column with 10 axial nodes, subjected to the typical operating limits at the edge of the thermal-mechanical operating envelope, shown in Figure 3-3.

[[

]]

Figure 3-3 Representative Thermal-Mechanical Envelope for GNF2

In this case, [[]] At each of three limiting points on the envelope of Figure 3-3, the volume % of the fuel column that exceeds the eutectic temperature was calculated, assuming a parabolic radial temperature distribution for each node, and the results are shown in Figure 3-4.

[[

]]

Figure 3-4 Limiting Case of Fuel Fraction Above Eutectic Temperature

It can be seen from these results that even at the maximum anticipated operational LHGR, only a small fraction of the fuel column, [[]] in this case, is [[

]] Of that [[]], only a small fraction thereof is [[]] at these limiting conditions. Figure 3-5 illustrates to scale the regions of the fuel that experience temperatures [[]] at the limiting exposure of [[]].
[[]]

]]

Figure 3-5 Region of Fuel Above Eutectic at Limiting LHGR and Exposure

To further illustrate the conditions at the predicted highest temperature node at the highest temperature condition, the maximum centerline temperature predicted at that location is [[]], at which temperature the corresponding wt% liquid is approximately [[]], and about [[]] of the volume of this node is above the eutectic temperature. Even in this worst-case node, the total amount of liquid predicted is [[]]

]]

Furthermore, the liquid phase (more accurately called the vitreous phase) retains some resistance to deformation at temperatures above the eutectic temperature. Because the as-fabricated fuel pellets contain some vitreous phase even at room temperature, there is a continuous change in the material properties of the additive phase with increasing temperature, and the eutectic temperature, while representing the temperature at which a pure crystalline additive would melt, has no such meaning with a vitreous additive. Instead, the eutectic temperature represents the temperature at which UO₂ is expected to have any solubility in the vitreous phase, and there is not an associated step change in the material properties of the aluminosilicate itself.

The preceding examples are illustrations intended to show that in aluminosilicate additive fuel the high temperature mechanical stability is not exceptionally dissimilar to standard UO₂ fuel, and there is little risk of significant geometric redistribution of the fuel column due to the liquid that can be present in additive fuel.

3.3 REACTIVITY INSERTION ACCIDENT (RIA) CHARACTERISTICS

Reactivity Insertion Accident (RIA) testing of additive fuel has demonstrated that additive fuel meets applicable licensing requirements and furthermore shown there is no measurable RIA fuel performance penalty suffered by additive fuel compared to standard non-additive fuel. A total of 30 rods, including standard fuel as well as fuel with a variety of additive compositions and concentrations, were tested in the Nuclear Safety Research Reactor (NSRR) at the Japan Atomic Energy Research Institute. In these tests, the fuel evaluated included high and low additive concentrations [[]] and A and B additive compositions [[]]. These additive types apply to the range of additive compositions considered in this Report, and the “low” additive concentration is equal to the [[]] for licensing in this Report. The deposited energy examined in this testing program ranged from [[]] and the results summarized in Figure 3-6.

[[

]]

Figure 3-6 RIA Testing Results

All of the additive fuel tested, as well as the GE non-additive fuel tested, exceeded the NSRR standard rod failure threshold of 260 cal/gUO₂ and was at least comparable to the GE standard rod threshold of [[]]. The failure threshold was shown with certainty to be at [[]] for fuel with the highest kaolin additive concentration and for standard fuel, and was shown to be around [[]]. Testing of rods with [[]], resulted in better resistance to rod failure than identical failed tests for higher concentrations, indicating that the failure thresholds indicated above for [[]] additive are conservative assessments of the RIA resistance of additive fuel of the type proposed. Additive fuel was also observed, where readily comparable, to exhibit less fragmentation than standard fuel.

3.4 IN-REACTOR DENSIFICATION

Additive fuel pellet in-reactor densification (and swelling) behavior is expected to be unchanged with respect to standard UO₂ fuel. Prior manufacturing experience indicates that there is little difference in the sintering kinetics and therefore densification behavior of additive fuel. A limited amount of in-reactor testing also supports this conclusion. [[

]], so it is also expected that, much like GNF non-additive fuel [Reference 4], additive fuel will be inherently resistant to significant in-reactor densification.

Because the additive fuel densification behavior is so similar to that of standard UO₂ fuel, the methodology for densification testing and qualification of additive fuel will follow the same approved methodology for standard UO₂ fuel as described in NEDE-33214P-A. [[

]]

3.5 EFFECT ON ALTERNATE SOURCE TERM

The alternate source term used in plant licensing should apply equally well to additive and non-additive fuel. The source term is detailed in NUREG-1465, which was introduced in 1995 to provide for a more realistic estimate of the radiological species released to containment in the event of a severe reactor accident involving substantial meltdown of the core. That document describes the specific nuclide types, quantities, chemical form, phase and timing of release into containment. The resulting source term is used in safety analyses for the design of plant systems and for plant licensing. [[

]] The alternate source term assumes that 95% of the released iodine is in the chemical form of CsI, with the remainder as volatile elemental iodine (I₂) and

organoiodides, e.g. CH₃I. These assumptions reduce the total amount of volatile iodine available to leave containment because CsI is highly soluble in water. Additionally, the source term model assumes the pH of water within the containment to be above 7. This constraint minimizes the irradiation-induced conversion of ionic iodine present in pools of water and on wet surfaces to elemental iodine. The analysis of such containment water assumes that the released Cs forms CsOH, which contributes to maintaining the pH at values greater than 7. This analysis assumes only a portion of the released Cs is converted to CsOH. Therefore, a significant amount of Cs needs to be released from the fuel to the containment for these assumptions to remain valid. [[

]]

- The amount of silica to be added is [[

]]

- The additive resides on the grain boundaries and is essentially insoluble in the grain matrix. The intergranular silica may [[

]]

satisfy the NUREG-1465 criteria in the event of an accident because:

[[

]]

Therefore, the alternate source term assumptions used in design of plant systems and plant licensing should not be affected by the use of additive fuel.

3.6 LONG TERM FUEL STORAGE

For long-term storage, the concerns are the initial conditions at the start of storage (i.e. end of reactor operation), response during storage, and response to a cladding failure during storage. The initial conditions of interest include: the rod internal pressure, cladding corrosion and crud (impacts decay heat transfer and thus temperature during storage), cladding hydrogen concentration and morphology, and cladding strain. The presence of additive will have no impact on these parameters.

The response during storage includes possible additional cladding creep and corrosion and changes in hydride morphology resulting in hydrogen assisted or delayed hydrogen-cracking failure or reduced ductility or more specifically reduced seismic margin. Again, for the same initial conditions, the presence of additive will have no impact on these responses.

Fuel temperatures in the spent fuel pool will be near the temperature of the spent fuel pool water or very low. Fuel temperatures in dry storage are dictated by the specific loading of the dry storage cask, which depend on burnup and time after shutdown. The current regulations require the fuel temperatures to remain below 400°C in dry storage (Reference 5). For both of these cases, the fuel temperatures are below the melting temperature of additive fuel, so neither fuel relocation nor other phenomena associated with fuel melting are concerns for long term storage.

The concern after failure is fuel dispersal. For dry storage, including cask drying for transportation, dispersal will be negligible due to the relatively low temperatures and lack of water flow over the fuel. Because the temperatures are below the eutectic temperature of additive fuel, additive fuel will have no impact on this already negligible dispersal. Similarly, for wet storage, dispersal will be negligible due to the very low temperatures and very slow flow velocities (driven by convection only). Additive fuel will have no affect on this negligible dispersal.

4.0 QUALIFICATION DATA

GNF has conducted several experimental programs to investigate additive fuel behavior. These investigations were performed in commercial BWRs as well as test reactors. The experimental measurements include fission gas release, cladding diametral deformation and fuel temperature and rod internal pressure. Comparison of the PRIME code predictions with these measured data are discussed in the following subsections.

4.1 QUALIFICATION DATASET

GNF additive fuel rods have been successfully irradiated in power reactors since 1977, first in low-power segmented rod bundles and later in unrestricted LTAs. The experimental programs selected for PRIME additive fuel model qualification are briefly described in the following subsections.

4.1.1 [[]] – HALDEN RAMP TESTS

Five Lead Use Assemblies (LUAs) were fabricated by GE in 1984 and loaded into [[]] for irradiation. To achieve segment exposures in the target range, the LUAs were irradiated in [[]] The segments were generally representative of GE8 (8x8) fuel rods. All segments were comprised of nominally 0.483 inch outside diameter cladding. The nominal active fuel length was 26.29 inches, and the nominal plenum volume was 0.696 in³. Some of the segments contained 8 w/o Gd₂O₃-UO₂ with low levels of aluminosilicate additive.

After the [[]], some segments were transported to the Halden test reactor in Norway for bump testing. In this case, the segments were placed in a test assembly and incubated for ~2-20 days at relatively low power levels (~6.0 - 7.5 kW/ft). After the incubation period, the power level in the test assembly was increased to elevate the segment power levels to values near the design and licensing basis power-exposure envelope. The test segments were then held at the bump power levels for ~30 days to ensure that equilibrium fission gas release conditions were achieved. At the end of Halden bump testing, segments were punctured for fission gas release measurements. The results from segments used for PRIME03 additive model qualification are summarized in Table 4-1.

Segment ID	Exposure, GWd/tU	GD ₂ O ₃ Concentration, w/o	Additive Concentration, w/o	Measured FGR, %	PRIME03, FGR %
[[
]]

Table 4-1 Model Qualification Cases from [[]]-Halden Ramp Tests

4.1.2 HALDEN STEADY-STATE (THERMAL RIGS) TESTS

Standard UO₂ fuel and 2500 wppm or 0.25 wt.% natural clay additive fuel rods were irradiated in Halden in the [[]]. Test variables were pellet-clad gap, additive type and power. Test rods were instrumented with fuel centerline thermocouples, fuel column elongation sensors and gas pressure sensors. The rigs were inserted in 1985 and the last one was discharged in 1996. Table 4-2 summarizes the cases selected for PRIME03 additive model qualification with measured and calculated FGR.

Tests	Exposure, GWd/tU	Additive Concentration, w/o	Fuel Centerline Temperature	Measured Fission Gas Release, %	PRIME03 FGR, %
[[
]]

Table 4-2 Model Qualification Cases from Halden Steady-State (Thermal Rigs) Tests

4.1.3 [[]]-HALDEN RAMP TESTS

Fuel rod segments containing [[]] aluminosilicate additives at the [[]] (by weight) levels, as well as standard UO₂, in non-barrier cladding were base irradiated [[]]. The PCI resistance of the additive fuels, relative to

that of standard UO₂ was determined by power ramp tests performed in the Halden Reactor. Power ramp testing of the segments was started in May 2001 in the Halden reactor in the assembly [[]]. All testing was completed by the end of June 2001. Candidate rods selected for PRIME03 additive model qualification are summarized in Table 4-3.

Segment Serial Number	Halden Test	Pre/Post Ramp Test Exposure, GWd/tU	Additive Concentration, ppm	Measured Fission Gas Release, %	PRIME03 FGR, (%)	Max. Cladding Strain, %
[[
]]

Table 4-3 Model Qualification cases from [[]]-Halden Ramp Tests

4.1.4 NFD HALDEN THERMAL RIG TESTS

GNF participated in a joint research program, termed the NFD Halden thermal rig tests, with the Japanese Utility Group to understand additive fuel behavior. Table 4-4 summarizes for selected rods, measured and calculated fission gas release (FGR) and end-of-life (EOL) rod internal pressure for these tests.

Fuel Type	Exposure (MWd/t)	Measured FGR (%)	PRIME03 FGR(%)	Measured EOL Pressure, psia	PRIME03 EOL Pressure, psia
[[
]]

Table 4-4 Model Qualification cases from NFD-Halden Thermal Rig Tests

4.1.5 NUPEC(JNES) STEP3 LUA TESTS

PRIME03 additive model qualification candidate rods from NUPEC(JNES) STEP3 LUA Tests are summarized in Table 4-5. Measured and PRIME03 calculated FGR data are also summarized in Table 4-5

Fuel Type	EOL Rod Average Exposure (GWd/t)	Measured FGR (%)	PRIME03 FGR (%)	Measured $\Delta D/D$, %	PRIME03 $\Delta D/D$, %
[[
]]

Table 4-5 Model Qualification cases from NUPEC(JNES) STEP3 LUA Tests

4.1.6 [[]]-LUA TESTS

Eight LUAs representative of GE14 fuel and designed for high burnup exposures started irradiation in [[]]. The LUAs included both full and segmented rods with aluminosilicate additive fuel pellets and utilized improved cladding and spacer materials. Three full-length rods and four segmented rods (9 total rod segments) from this LUA program were transported from [[]] for rod puncturing and fission gas release measurements. The rods contained UO₂ plus aluminosilicate additive at concentrations of either [[]]

The results used for PRIME03 additive model qualification are summarized in Table 4-6.

Rod/Segment ID	Exposure, GWd/tU	Additive Concentration, w/o	Measured FGR%	PRIME03 FGR%
[[
]]

Table 4-6 Model Qualification Cases from [[**]]**

4.1.7 PRIME QUALIFICATION RESULTS

Fuel centerline temperature, fission gas release, rod internal pressure and cladding diametral strain for additive fuel were compared with non-additive cases previously used to qualify PRIME03. PRIME03 additive qualification results are discussed in the following subsections.

4.1.7.1 FUEL CENTERLINE TEMPERATURE QUALIFICATION

Additive fuel centerline data are compared with the PRIME03 non-additive qualification dataset to identify any significant bias in the additive data. An overall comparison of predicted and measured fuel centerline temperature for both the additive and non-additive cases is shown in Figure 4-1. The ratios of predicted/measured fuel centerline temperature as a function of exposure are presented in Figure 4-2. Fuel centerline temperature for the additive cases is well within the scatter of the PRIME03 non-additive qualification data and independent of fuel exposure.

[[

]]

Figure 4-1 Predicted versus Measured Fuel Temperature

[[

]]

Figure 4-2 Predicted/Measured Fuel Temperature versus Exposure

4.1.7.2 FISSION GAS RELEASE QUALIFICATION

Figure 4-3 and Figure 4-4 compares predicted and measured values of fission gas release for the PRIME03 dataset and the additive fuel dataset. The additive fission gas release data are well within the scatter of the non-additive data. Figure 4-4 shows no bias with exposure for the additive fuel fission gas release when compared with non-additive fuel.

[[

]]

Figure 4-3 Predicted versus Measured Fission Gas Release

[[

]]

Figure 4-4 Predicted/Measured Fission Gas Release versus Exposure

4.1.7.3 FUEL ROD INTERNAL PRESSURE QUALIFICATION

Comparisons of predicted and measured rod internal pressure for additive and non-additive fuel are presented in Figure 4-5 and Figure 4-6. No substantive deviation in PRIME03 prediction for the additive fuel internal pressure is observed when compared with non-additive fuel.

[[

]]

Figure 4-5 Predicted versus Measured Fuel Rod Internal Pressure

[[

]]

Figure 4-6 Predicted-Measured Rod Internal Pressure versus Exposure

4.1.7.4 FUEL CLADDING STRAIN QUALIFICATION

PRIME03 predictions of cladding strain for both the non-additive case and additive fuel rods are shown in Figure 4-7 and Figure 4-8. No significant difference in PRIME03 predictions for additive and non-additive fuel is observed.

[[

]]

Figure 4-7 Predicted versus Measured Cladding Diametral Strain

[[

]]

Figure 4-8 Predicted-Measured Cladding Diametral Strain

4.2 PRIME QUALIFICATION CONCLUSIONS

Fuel centerline temperatures, fission gas release and rod internal pressure prediction for the additive fuels are well within the scatter of non-additive data, and no significant bias with exposure is observed. The addition of additive cases does not change PRIME03 model uncertainties.

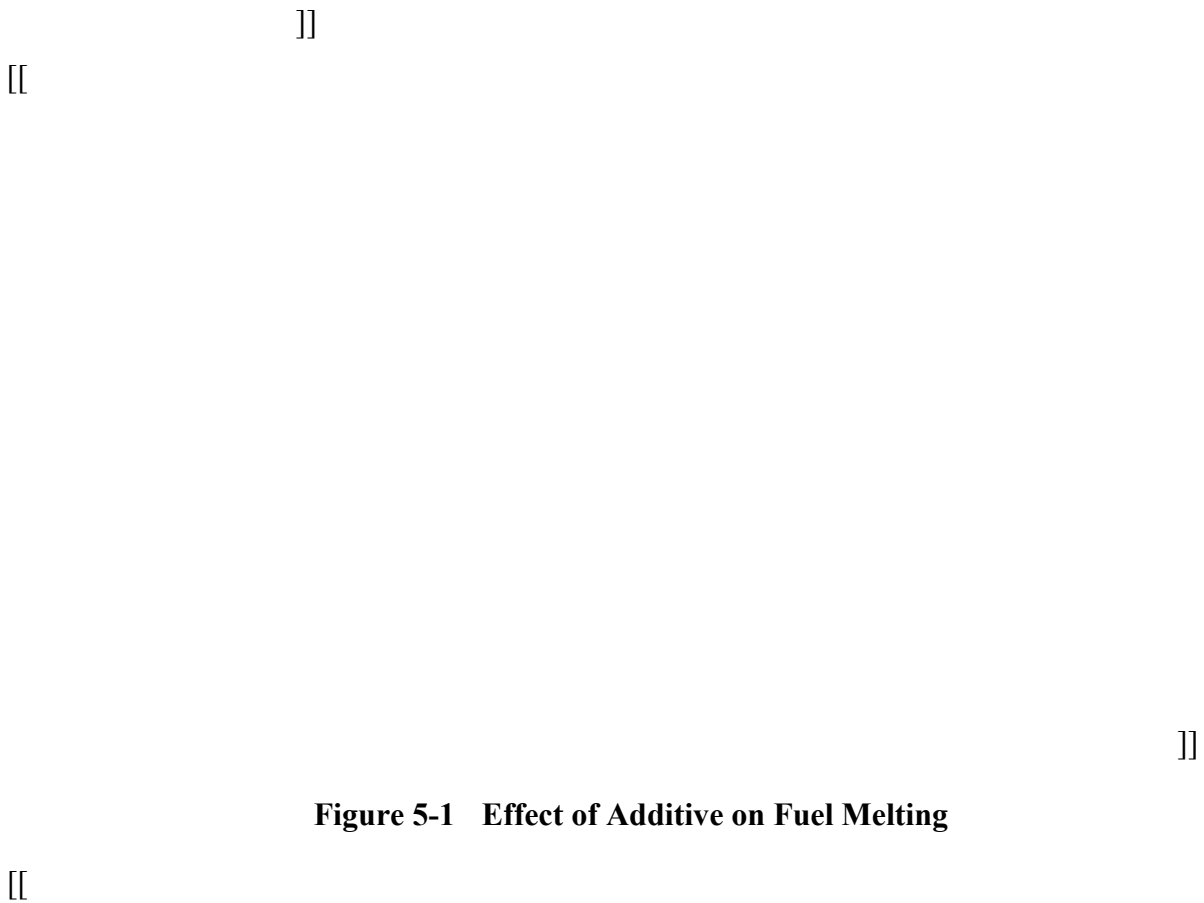
5.0 LICENSING CRITERIA ASSESSMENT

The material properties discussed in Section 2.1 have been implemented into the GNF thermal mechanical engineering computer code PRIME. PRIME has been submitted to the NRC for review and approval. The intent of this section is to show the effect of additive on the design bases for each of the fuel system damage, failure and coolability criteria, established in the Standard Review Plan 4.2 in NUREG-0800, relative to standard fuel by analyzing the limiting fuel design characteristics with the proposed range of additive and comparing the results to standard fuel with methodologies defined in GESTAR II. It will be shown for each licensing criterion that additive fuel is equivalent to or better than current UO₂ fuel. This assessment forms the basis for demonstrating that GESTAR II is also applicable to additive fuel.

The demonstration calculations included herein are based on the GNF2 fuel design analyzed using PRIME. The GNF2 fuel design is chosen because the design has the highest licensed linear heat generation rate (LHGR) in the current GNF fuel product line. The values shown in this section are representative of additive fuel and not the actual limits. The analysis reflects the current criteria, and it should be noted that other criteria changes may require the limits to be modified to insure compliance. The methodology described is consistent with the previously submitted PRIME application report.

5.1 FUEL MELTING

As described in Section 2.1 the fuel melting behavior of additive fuel is different than for standard fuel. However, the method of analysis used to protect standard fuel can be conservatively applied to additive fuel by [[



]]

5.2 FUEL ROD INTERNAL PRESSURE

Fuel rod internal pressure is limited by the licensing requirement that there [[

]]

To demonstrate the effect of additive in the PRIME calculation of fuel rod internal pressure, the GNF2 fuel rod design was analyzed with and without additive. Input parameters that affect the fission gas model have been conservatively chosen. For example, [[

]]

[[

]]

Figure 5-2 Effect of Additive on Fuel Rod Internal Pressure

5.3 CLADDING PLASTIC STRAIN

Analyses are performed for each rod type to determine the values of maximum overpower (Mechanical Overpower) magnitudes [[

]]

Additive fuel will be much more compliant than standard fuel during AOOs due to the high fuel temperatures, and will reduce the cladding strain and enhance margin relative to this licensing criterion. To demonstrate the impact, a typical mechanical overpower analysis, as described above, was performed for fuel with and without additive to compare the levels of permanent cladding strain as a function of exposure. Figure 5-3 shows the results.

[[

]]

Figure 5-3 Effect of Additive on Cladding Permanent Strain

As can be seen by the figure, the presence of additive [[

]]

5.4 CLADDING FATIGUE PLUS CREEP RUPTURE LIMIT

The cladding fatigue analysis also reflects operation [[

]]

To demonstrate the effect of additive on the fatigue life, additive and standard fuels were analyzed with PRIME. The standard analysis used at GNF by procedure also includes [[

]]

Table 5-1 shows the results for both the standard fuel and additive fuel case.

[[

]]

Table 5-1 Fraction of Allowable Fatigue Lifetime Expended

[[

]] Additive

fuel has minimal impact relative to the margin for non-additive fuel and satisfies the cladding fatigue design/licensing limit of [[

]] In general, additive will reduce cladding strains associated with pellet cladding mechanical interaction and improve fatigue life.

5.5 CLADDING CREEP COLLAPSE

Historically, GNF has performed a cladding creep collapse analysis for each new fuel design. This calculation was deliberately conservative to address uncertainties in GNF fuel rod performance that existed at the time the methodology was reviewed and approved by the NRC.

[[

]] An LTR documenting the revised methodology, together with a bounding calculation intended to address GNF2 and future fuel designs, was submitted to and approved by the NRC (NEDC-33139P-A). Upon approval of the LTR, a creep collapse analysis was no longer required for a new fuel design unless the bounding analysis in the LTR did not apply to that design.

Based upon the characterized densification and fission gas release performance of GNF additive fuel relative to non-additive fuel, the revised methodology is applicable to additive fuel. Since additive fuel is otherwise identical to non-additive fuel, the bounding analysis in NEDC-33139P-A is applicable to additive fuel and additional consideration of creep collapse is not required.

5.6 LOCA\STABILITY\CORE TRANSIENTS

As discussed above additive fuel at the concentrations being considered has been shown to have only a small effect on the fuel thermal mechanical response. This suggests evaluation of core events such as LOCA, various transient events associated with reload licensing, and core stability are essentially insensitive to the differences as calculated by PRIME and therefore do not necessarily require explicit treatment in those analyses. The claim of insensitivity can be made on the basis of the magnitudes of the changes due to the presence of the additives relative to the stated uncertainties of the analysis codes.

For example LOCA evaluations using PRIME plus TRACG analysis codes require

[[

]]

[[

]]

Table 5-2 Uncertainty in Melt Margin Analysis

Similarly, LOCA, transient, and stability analyses use the input [[

]], respectively.

[[

]]

Table 5-3 Effect of Additive on High-Power Gap Conductance

[[

]]

Table 5-4 Effect of Additive on Low-Power Gap Conductance

[[

]]

[[

]]

Table 5-5 Effect of Additive on Fuel Centerline Temperature

This section has demonstrated that the magnitude of the differences due to the addition of a small amount of additive to UO₂ fuel is insignificant to parameters affecting LOCA, Transient, and Stability analysis. For this reason, explicit analysis of those transients for additive fuel is not included in this report. Fuel designs containing additive will be licensed following the normal new fuel and reload licensing procedures.

5.7 IMPACT ON NUCLEAR DESIGN REQUIREMENTS

General Design Criterion (GDC) 11 stipulates that the reactor core and associated coolant systems shall be designed so that in the power operating range the net effect of the prompt inherent nuclear feedback characteristics tends to compensate for a rapid increase in reactivity. To confirm compliance with GDC 11, key nuclear dynamic parameters, or reactivity coefficients, are evaluated when new fuel designs are developed. For BWR fuel, the key reactivity coefficients are: 1) the moderator void coefficient, 2) the moderator temperature coefficient, 3) the Doppler coefficient and 4) the prompt power coefficient. The impact of introducing additive fuel on these key reactivity coefficients has been evaluated and confirmed to not impact the nuclear dynamic parameters.

The absorption cross section for aluminosilicate additive is very small in relation to the fuel. The primary effect of introducing additive is to displace a small amount of UO₂ which does tend to make reactivity coefficients less negative. Infinite lattice studies were performed to examine the impact on the change in reactivity associated with a change core state (e.g. moderator void) due to the reduced fuel density. The impact on reactivity change is small and does not affect a fuel assembly's inherent compliance with GDC 11 in light of the large margins.

General Design Criteria 26 stipulates that the reactivity control system shall be capable of maintaining the reactor subcritical under cold conditions with sufficient margin to account for equipment malfunctions such as stuck control rods. Adequate cold shutdown margin (CSDM) is assured through cycle specific 3D analyses. Here again, the primary effect of introducing additive fuel is to reduce the fuel density slightly which has a small effect on core reactivity and control rod worth in the cold condition; however, the reduced fuel density will be explicitly modeled in generating nuclear libraries as part of cycle specific reload analysis for fuel

containing aluminosilicate additive. As such, compliance with GDC 26 is assured on a cycle-specific basis.

5.8 LICENSING CRITERIA CONCLUSION

The assessments above confirm that the impact of additive fuel on licensing analysis for GNF fuel designs are negligible and do not impact the relevant behavior or characteristics.

Furthermore, the same application methodologies used for licensing standard fuel as defined in GESTAR II are applicable to additive fuel, and no changes in the criteria are required, [[

]]

6.0 OPERATING EXPERIENCE

6.1 BACKGROUND

GNF additive fuel has been irradiated in power reactors in the United States and abroad since 1977. In that time, data relating to pellet properties and operating characteristics has been obtained. Figure 6-1 summarizes this experience.

	Reactor	Description	Exposure Gwd/MTU	1970	1975	1980	1985	1990	1995	2000	2005	2010	
Test Reactors	GETR	66 rods	80 (max)			█							
	R2												
	Halden												
	NSRR												
Power Reactors (SRB, LTA, LUA)	Millstone	54 rods	25			█							
	Monticello QC-1												
	Caorso	5 bundles	35			█							
	Duane Arnold	5 bundles	40			█							
	Forsmark-1	4 bundles	40						█				
	Fukushima-1	2 bundles	50					█					
	Gun-C	8 bundles (4 bundles)	68 (80)						█			█	
	Reload Fuel	BWRs-Japan	All (U,Gd)O ₂ rods	---						█		█	

Figure 6-1 Additive Fuel Operating History Summary

Of the additive fuel rods that have operated in power reactors, the earliest of rods were part of the segmented rod bundle (SRB) program and consisted of specially designed segmented rods with up to [[]] These early rods attained up to approximately

[[]] exposure and were retrieved for hot cell examination and further testing (e.g. ramp testing). Later, restricted lead test assemblies (LTAs) were inserted into [[]] and achieved approximately [[]] exposure. The LTAs contained segmented rods and full-length rods. The segmented rods were retrieved for hot cell examination and further testing. Most recently, 10x10 designs, GE12 and GE14, containing from [[]] have operated as unrestricted lead use assemblies (LUAs) in the [[]] These LUAs contained segmented and full-length rods. The [[]] have achieved approximately [[]] exposure. Seven rods from those LUAs have been retrieved for hot cell examination and further testing in 2009. Some of the [[]] bundles have been re-inserted into the reactor to accumulate more exposure before examination. Fuel rod segments retrieved from the SRB bundles and [[]] have been ramp tested.

6.2 STEADY STATE IRRADIATION

The goal of the Lead Use and Lead Test (LUA/LTA) program was to provide irradiated fuel rods material for subsequent ramp testing to determine the minimum amount of additive that is still effective in guarding against PCI. The additive displaces uranium, so, there is economic incentive to limit the amount. More importantly, though, lower concentrations will reduce the impact on fuel fabrication and fuel properties making the transition to additive fuel more simple. As discussed above the LUAs contained segmented rods having concentrations ranging from [[]] fabricated from a [[]] The bundles operated as standard 10x10 bundles with the exception that power was kept low to preclude any pre-conditioning effects that could contribute enhanced performance in subsequent ramp testing. The exposure of the tested segments ranged from [[]]

In addition to the ramp testing described in section 6.3, examinations of the fuel and cladding structure were performed. These examinations confirm that [[]]

]]

Both the additive and non-additive pellets contained [[

]]

The most recent LUA application of additive fuel was as part of an ongoing ultra-high burn up program being conducted at [[]]. Eight fuel bundles were manufactured in 1999 containing additive UO₂ fuel rods consisting of [[]] at concentrations of [[]]. The fuel was fabricated at the GNF Wilmington fuel plant and exhibited characteristics similar to additive fuel produced in the past for properties characterization and performance testing. Specifically, the fuel density and grain size are consistent with past additive fuel and the composition and

6.3 RAMP TESTING AND DEMONSTRATED PCI RESISTANCE

[[

]]

Figure 6-2 Additive Fuel Ramp Testing Results

The SRB rods were ramp tested in the Studsvik R2 test reactor. The peak power achieved during testing was limited to 18 kW/ft due to the capabilities of the reactor. [[

]] The rod segments tested contained additive concentrations of

[[

]] The

[[rods were ramp tested in Halden test reactor. The peak power achieved during testing was approximately 16 kW/ft, again limited by the capability of the test reactor. A total of twelve rods were tested (all without an inner Zirconium liner or barrier). Eight rods contained additive [[

]] and 4 rods with standard

UO₂. The four standard rods failed during testing, but none of the eight 10x10 additive rods failed. Figure 6-2 shows the additive PCI ramp test data results from the SRP and [[

]] programs superimposed over the standard UO₂ failure probability lines. [[

]]

Measurements of cladding diameter were made to determine the strain produced by the power ramps. [[

]]

[[

]]

The ramp test program of additive rods [[]] provided a valid assessment of PCI performance. The tests demonstrated the PCI resistance of additive fuel at [[

]] In other aspects, the behavior of additive and non-additive pellets were essentially equal.

Results of the ramp testing also demonstrated the outcome of operation of the additive fuel [[]] Following ramp testing, SEM investigation of transverse samples from three unfailed ramped additive rods were prepared and examined. [[

]]

In addition to the SEM examinations, the corresponding peak centerline and surface temperatures associated with each axial location were calculated using the PRIME model. The inputs required for the PRIME model were based on the power history of the fuel segments. All of the segmented fuel rods were base irradiated in the Forsmark-1 power reactor prior to insertion into the Halden Reactor for ramp testing. The power histories modeled in PRIME simulated the incubation period as well as the power ramp tests.

A summary of the segmented test rods can be seen below in Table 6.1.

	[[
Position from rod bottom (mm)			
Additive Concentration (ppm)			
Peak Exposure (MWd/MTU)			
LHGR (kW/ft)			
Peak Surface Temperature (°C)			
Peak Centerline Temperature (°C)			
Time Above 1550 °C (hours)]]

Table 6-1 Summary of Segmented Rods from Halden Ramp Testing

Furthermore, Figures (6-3) through (6-5) show the calculated temperature gradients as function of the pellet radius for each unfailed rod. [[

]]

[[

]]

Figure 6-3 Temperature Gradient of Rod Segment [[]]

[[

]]

Figure 6-4 Temperature Gradient of Rod Segment [[]]

[[

]]

Figure 6-5 Temperature Gradient of Rod Segment [[]]

[[

NEDO-33406 REVISION 2
NON-PROPRIETARY INFORMATION

]]

7.0 CONCLUSION

GNF desires to introduce aluminosilicate additive fuel pellets to increase fuel reliability and operational flexibility of nuclear fuel bundles and cores. Additive fuel has been successfully tested over a wide range of concentrations and compositions. In order to eliminate any deleterious effects on fuel economics or fuel properties, the amount of additive and the composition range proposed will be limited to the ranges indicated below.

Additive Fuel Range of Applicability			
	Concentration wt%	Composition SiO ₂ : Al ₂ O ₃ by wt	Fuel Design
Target Range	[[]]	[[]]	GE14, GNF2, new

As described in this report additive in the stated concentration range has a negligible effect on licensing limits as demonstrated by PRIME. Fuel designs incorporating additive can be licensed to the same or improved limits as designs with standard fuel with greater margin to failure mechanisms associated with pellet clad interaction. This additional margin will lead to more robust fuel that is more resistant to systemic in-core fuel failures.

In the proposed range, significant effects from the addition of aluminosilicate additive to the fuel pellet are limited to a few key characteristics: [[

]] The remaining fuel properties or behaviors such as [[
]] are insignificantly affected by additive. [[

]]

GNF has operated additive fuel in irradiation programs ranging from single rod segments to full bundle LUAs. The in-core experience has been valuable to provide fuel rods for property development as well as understanding in-core behavior. Average bundle exposures of up to [[

]] have been obtained. Fuel inspections at various points in exposure have indicated satisfactory operation. The LUA programs demonstrate the capability of additive fuel to perform as expected to the limits of licensed exposures common to current GNF fuel designs.

8.0 REFERENCES

1. The PRIME Model for Analysis of Fuel Rod Thermal – Mechanical Performance Part 1 – Technical Bases, Global Nuclear Fuel, Wilmington, NC: 2007 NEDC-33256P
2. The PRIME Model for Analysis of Fuel Rod Thermal – Mechanical Performance Part 2 – Qualification, Global Nuclear Fuel, Wilmington, NC: 2007 NEDC-33257P
3. The PRIME Model for Analysis of Fuel Rod Thermal – Mechanical Performance Part 3 – Application Methodology, Global Nuclear Fuel, Wilmington, NC: 2007 NEDC-33258P
4. Densification Testing, Global Nuclear Fuel, Wilmington, NC:2007 NEDE-33214P-A
5. Spent Fuel Project Office, Interim Staff Guidance – 11, Revision 3, Cladding Considerations for the Transportation and Storage of Spent Fuel